第 34 卷第 5 期
2018 年 5 月

无 机 化 学 学 报
CHINESE JOURNAL OF INORGANIC CHEMISTRY

Vol.34 No.5
981-988

由联苯三羧酸配体构筑的零维四核镍(Ⅱ)配合物和一维锰(Ⅱ)配位聚合物的合成、晶体结构及磁性质

黎 彧*,[1] 温炳松[2] 邹训重[1] 黄 宾[1] 邱文达[1] 张泽敏[1] 游 遨[1] 成晓玲*,[2]

([1]广东轻工职业技术学院生态环境技术学院,佛山市特种功能性建筑材料及其绿色制备技术工程中心,广州 510300)

([2]广东工业大学轻工化工学院,广州 510006)

摘要:采用水热方法,用 2 种联苯三羧酸配体 biphenyl-2,5,3′-tricarboxylate acid(H_3bptc)和 2-(4-carboxypyridin-3-yl)terephalic acid(H_3cptc)以及菲咯啉(phen)或 2,2′-联吡啶(2,2′-bipy)分别与 $NiCl_2\cdot 6H_2O$ 和 $MnCl_2\cdot 4H_2O$ 反应,合成了一个具有零维四核镍结构的配合物$[Ni_2(\mu_3\text{-Hbptc})(Hbptc)(phen)_3(H_2O)]_2\cdot 4H_2O$ (**1**)和一个基于三核锰单元的一维链状配位聚合物$\{[Mn_3(\mu_4\text{-cptc})_2(2,2'\text{-bipy})_2(H_2O)_4]\cdot 2H_2O\}_n$ (**2**),并对其结构和磁性质进行了研究。结构分析结果表明 2 个配合物均属于三斜晶系,$P\bar{1}$ 空间群。配合物 **1** 具有零维四核镍结构,而且这些四核镍单元通过 O–H···O 氢键作用进一步形成了三维超分子框架。而配合物 **2** 中存在一个中心对称的三核锰单元,这些三核锰单元又通过配体进一步连接成了一维链。研究表明,配合物 **1** 和 **2** 中相邻金属离子间存在反铁磁相互作用。

关键词:配位聚合物;氢键;三羧酸配体;磁性

中图分类号:O614.81+3;O614.71+1 **文献标识码**:A **文章编号**:1001-4861(2018)05-0981-08

DOI:10.11862/CJIC.2018.131

Syntheses, Crystal Structures, and Magnetic Properties of 0D Tetranuclear Nickel(Ⅱ) Coordination Compound and 1D Manganese(Ⅱ) Coordination Polymer Constructed from Biphenyl Tricarboxylic Acid

LI Yu*,[1] WEN Bing-Song[2] ZOU Xun-Zhong[1] HUANG Bin[1]

QIU Wen-Da[1] ZHANG Ze-Min[1] YOU Ao[1] CHENG Xiao-Ling*,[2]

([1]*School of Eco-Environmental Engineering, Foshan Research Center for Special Functional Building Materials and Its Green Preparation Technology, Guangdong Industry Polytechnic, Guangzhou* 510300, *China*)

([2]*School of Chemical Engineering and Light Industry, Guangdong University of Technology, Guangzhou* 510006, *China*)

Abstract: A 0D tetranuclear nickel(Ⅱ) coordination compound and a 1D manganese(Ⅱ) coordination polymer, namely $[Ni_2(\mu_3\text{-Hbptc})(Hbptc)(phen)_3(H_2O)]_2\cdot 4H_2O$ (**1**) and $\{[Mn_3(\mu_4\text{-cptc})_2(2,2'\text{-bipy})_2(H_2O)_4]\cdot 2H_2O\}_n$ (**2**), have been constructed hydrothermally using H_3bptc (H_3bptc=biphenyl-2,5,3′-tricarboxylate acid), H_3cptc (H_3cptc=2-(4-carboxypyridin-3-yl)terephalic acid), phen (phen=1,10-phenanthroline) or 2,2′-bipy (2,2′-bipy=2,2′-bipyridine), and nickel or manganese chlorides. Single-crystal X-ray diffraction analyses revealed that both compounds crystallize in the triclinic system, space group $P\bar{1}$. In compound **1**, two μ_3-Hbptc^{2-} ligands bridge alternately neighboring Ni(Ⅱ) ions to form a discrete tetranuclear nickel(Ⅱ) structure. These Ni_4 units are assembled to a 3D supramolecular framework through O–H···O hydrogen bond. In compound **2**, three neighboring Mn(Ⅱ) ions are bridged by four different μ_4-

收稿日期:2017-12-01。收修改稿日期:2018-03-17。

广东省高等职业院校珠江学者岗位计划资助项目(2015),广东省自然科学基金(No.2016A030313761),广东轻院珠江学者人才类项目(No.RC2015-001),生物无机与合成化学教育部重点实验室开放基金(2016),广东省高校创新团队项目(2017),国家自然科学基金(No.21701032),佛山市科技计划项目(No.2017AB003922)和广东轻院人才类项目(No.KYRC2017-0021,KYRC2017-0025)资助。

*通信联系人。E-mail:liyuletter@163.com,ggcxl@163.com

cptc^{3-} ligands, giving rise to a centrosymmetric trinuclear Mn(Ⅱ) subunit. The adjacent Mn_3 subunits are further linked by the cptc^{3-} blocks into a 1D chain. Magnetic studies for compounds **1** and **2** demonstrate an antiferromagnetic coupling between the adjacent metal centers. CCDC: 1588394, **1**; 1588395, **2**.

Keywords: coordination polymer; hydrogen bonding; tricarboxylic acid; magnetic properties

0 Introduction

In recent years, the rational design and assembly of coordination polymers has been of considerable interest due to their potential applications, architectures, and topologies[1-5]. Many factors, such as the coordination geometry of the metal centers, type and connectivity of organic ligands, stoichiometry, reaction conditions, template effect, presence of auxiliary ligands, and pH values can play the key role in the construction of the coordination networks[6-10]. The design and selection of the special ligands is very important in the construction of these coordination polymers.

Multi-carboxylate biphenyl ligands have been certified to be of great significance as constructors due to their strong coordination abilities in various modes, which could satisfy different geometric requirements of metal centers[7-9,11-16]. In order to extend our research in this field, we chose two biphenyl tricarboxylic acid ligands, biphenyl-2,5,3′ -tricarboxylate acid (H_3bptc) and 2-(4-carboxypyridin-3-yl)terephalic acid (H_3cptc) to construct novel coordination compounds. Both ligands possesses the following features: (1) they have three carboxyl groups that may be completely or partially deprotonated, inducing rich coordination modes and allowing interesting structures with higher dimensionalities; (2) they can act as hydrogen-bond acceptor as well as donor, depending upon the degree of deprotonation; (3) the free rotation of C-C single bonds between two the aromatic rings could form numbers of coordination geometries of metal centers; thus, it may ligate metal centers in different orientation.

Taking into account these factors, we herein report the syntheses, crystal structures, and magnetic properties of two Ni (Ⅱ) and Mn (Ⅱ) coordination compounds constructed from biphenyl tricarboxylic acid ligands.

1 Experimental

1.1 Reagents and physical measurements

All chemicals and solvents were of AR grade and used without further purification. Carbon, hydrogen and nitrogen were determined using an Elementar Vario EL elemental analyzer. IR spectra were recorded using KBr pellets and a Bruker EQUINOX 55 spectrometer. Thermogravimetric analysis (TGA) data were collected on a LINSEIS STA PT1600 thermal analyzer with a heating rate of 10 ℃·min^{-1}. Magnetic susceptibility data were collected in the 2 ~300 K temperature range with a Quantum Design SQUID Magnetometer MPMS XL-7 with a field of 0.1 T. A correction was made for the diamagnetic contribution prior to data analysis.

1.2 Synthesis of [Ni_2(μ_3-Hbptc)(Hbptc)(phen)$_3$(H_2O)]$_2$·4H_2O (1)

A mixture of $NiCl_2·6H_2O$ (0.047 g, 0.20 mmol), H_3bptc (0.057 g, 0.2 mmol), phen (0.040 g, 0.2 mmol), NaOH (0.016 g, 0.40 mmol), and H_2O (10 mL) was stirred at room temperature for 15 min, and then sealed in a 25 mL Teflon-lined stainless steel vessel, and heated at 160 ℃ for 3 days, followed by cooling to room temperature at a rate of 10 ℃·h^{-1}. Green block-shaped crystals of **1** were isolated manually, and washed with distilled water. Yield: 45% (based on H_3bptc). Anal. Calcd. for $C_{66}H_{46}Ni_2N_6O_{15}$(%): C 61.91, H 3.62, N 6.56; Found (%): C 61.75, H 3.60, N 6.61. IR (KBr, cm^{-1}): 3 318w, 2 924m, 1 714w, 1 587s, 1 564s, 1 517m, 1 471w, 1 424m, 1 407w, 1 373w, 1 216w, 1 147w, 1 100w, 1 042w, 985w, 927w, 852w, 805w, 776w,724m, 643w, 516w.

1.3 Synthesis of {[Mn_3(μ_4-cptc)$_2$(2,2′-bipy)$_2$(H_2O)$_4$]·2H_2O}$_n$ (2)

A mixture of $MnCl_2·4H_2O$ (0.059 g, 0.30 mmol),

H_3cptc (0.057 g, 0.2 mmol), 2,2′-bipy (0.047 g, 0.3 mmol), NaOH (0.024 g, 0.60 mmol), and H_2O (10 mL) was stirred at room temperature for 15 min, and then sealed in a 25 mL Teflon-lined stainless steel vessel, and heated at 160 ℃ for 3 days, followed by cooling to room temperature at a rate of 10 ℃·h^{-1}. Yellow block-shaped crystals of **2** were isolated manually, and washed with distilled water. Yield: 62% (based on H_3cptc). Anal. Calcd. for $C_{48}H_{40}Mn_3N_6O_{18}$(%): C 49.97, H 3.49, N 7.28; Found(%): C 50.14, H 3.51, N 7.23. IR (KBr, cm^{-1}): 3 057w, 1 598m, 1 569s, 1 471w, 1 430w, 1 373s, 1 262w, 1 170w, 1 153w, 1 048w, 1 031w, 1 014w, 933w, 904w, 868w, 852w, 810w, 765m, 730w, 707w, 649w, 551w. The compounds are insoluble in water and common organic solvents, such as methanol, ethanol, acetone, and DMF.

1.4 Structure determinations

Two single crystals with dimensions of 0.25 mm×0.22 mm×0.21 mm (**1**) and 0.26 mm×0.24 mm×0.23 mm (**2**) were analyzed at 293(2) K on a Bruker SMART APEX Ⅱ CCD diffractometer with Mo $K\alpha$ radiation (λ =0.071 073 nm). The structures were solved by direct methods and refined by full matrix least-square on F^2 using the SHELXTL-2014 program[17]. All non-hydrogen atoms were refined anisotropically. All the hydrogen atoms were positioned geometrically and refined using a riding model. A summary of the crystallography data and structure refinements for **1** and **2** is given in Table 1. The selected bond lengths and angles for compounds **1** and **2** are listed in Table 2. Hydrogen bond parameters of compounds **1** and **2** are given in Table 3 and 4.

CCDC: 1588394, **1**; 1588395, **2**.

2 Results and discussion

2.1 Description of the structure

2.1.1 $[Ni_2(\mu_3\text{-Hbptc})(Hbptc)(phen)_3(H_2O)]_2\cdot 4H_2O$ (**1**)

Single-crystal X-ray diffraction analysis reveals

Table 1　Crystal data for compounds 1 and 2

Compound	1	2
Chemical formula	$C_{66}H_{46}Ni_2N_6O_{15}$	$C_{48}H_{40}Mn_3N_6O_{18}$
Molecular weight	1 280.51	1 153.68
Crystal system	Triclinic	Triclinic
Space group	$P\bar{1}$	$P\bar{1}$
a / nm	1.243 18(6)	0.719 34(4)
b / nm	1.422 15(10)	1.023 41(5)
c / nm	1.662 89(11)	1.739 84(11)
α / (°)	95.289(6)	96.993(5)
β / (°)	96.231(5)	101.237(5)
γ / (°)	108.755(5)	106.819(5)
V / nm^3	2.742 1(3)	1.180 71(13)
Z	2	1
F(000)	1 320	589
θ range for data collection / (°)	3.244~25.049	3.409~25.050
Limiting indices	$-14 \leqslant h \leqslant 14, -16 \leqslant k \leqslant 16, -19 \leqslant l \leqslant 15$	$-8 \leqslant h \leqslant 8, -12 \leqslant k \leqslant 12, -18 \leqslant l \leqslant 20$
Reflection collected, unique (R_{int})	17 820, 9 694 (0.061 9)	7 235, 4 178 (0.031 6)
D_c / (g·cm^{-3})	1.551	1.623
μ / mm^{-1}	0.768	0.876
Data, restraint, parameter	9 694, 0, 804	4 178, 0, 340
Goodness-of-fit on F^2	1.039	1.060
Final R indices [$I \geqslant 2\sigma(I)$] R_1, wR_2	0.074 3, 0.153 2	0.043 8, 0.081 8
R indices (all data) R_1, wR_2	0.134 7, 0.196 3	0.061 6, 0.091 5
Largest diff. peak and hole / (e·nm^{-3})	1 173 and −461	426 and −560

Table 2 Selected bond lengths (nm) and bond angles (°) for compounds 1 and 2

1					
Ni(1)-O(1)	0.207 9(3)	Ni(1)-O(2)A	0.207 0(4)	Ni(1)-N(1)	0.212 2(4)
Ni(1)-N(2)	0.207 9(5)	Ni(1)-N(3)	0.207 3(5)	Ni(1)-N(4)	0.211 8(5)
Ni(2)-O(6)	0.204 9(4)	Ni(2)-O(7)	0.221 2(4)	Ni(2)-O(8)	0.211 7(4)
Ni(2)-O(13)	0.202 8(4)	Ni(2)-N(5)	0.206 9(5)	Ni(2)-N(6)	0.205 9(5)
O(2)A-Ni(1)-N(3)	98.30(17)	O(2)A-Ni(1)-N(2)	88.22(18)	N(3)-Ni(1)-N(2)	170.67(18)
O(2)A-Ni(1)-O(1)	88.08(14)	N(3)-Ni(1)-O(1)	96.01(15)	N(2)-Ni(1)-O(1)	90.84(16)
O(2)A-Ni(1)-N(4)	174.09(17)	N(3)-Ni(1)-N(4)	78.83(19)	N(2)-Ni(1)-N(4)	94.05(19)
O(1)-Ni(1)-N(4)	97.32(16)	O(2)A-Ni(1)-N(1)	87.61(16)	N(3)-Ni(1)-N(1)	94.15(19)
N(2)-Ni(1)-N(1)	79.39(19)	O(1)-Ni(1)-N(1)	169.44(18)	N(4)-Ni(1)-N(1)	87.46(17)
O(13)-Ni(2)-O(6)	91.43(18)	O(13)-Ni(2)-N(6)	103.13(18)	O(6)-Ni(2)-N(6)	95.08(19)
O(13)-Ni(2)-N(5)	91.40(19)	O(6)-Ni(2)-N(5)	174.41(19)	N(6)-Ni(2)-N(5)	79.58(19)
O(13)-Ni(2)-O(8)	156.13(17)	O(6)-Ni(2)-O(8)	83.04(17)	N(6)-Ni(2)-O(8)	100.49(18)
N(5)-Ni(2)-O(8)	96.23(18)	O(13)-Ni(2)-O(7)	95.71(17)	O(6)-Ni(2)-O(7)	89.44(17)
N(6)-Ni(2)-O(7)	160.49(19)	N(5)-Ni(2)-O(7)	95.08(18)	O(8)-Ni(2)-O(7)	61.17(16)
2					
Mn(1)-O(1)	0.210 2(2)	Mn(1)-O(5)A	0.214 6(2)	Mn(1)-O(7)	0.213 2(2)
Mn(1)-N(1)A	0.226 7(3)	Mn(1)-N(2)	0.230 1(3)	Mn(1)-N(3)	0.232 3(3)
Mn(1)-O(2)	0.220 2(2)	Mn(1)-O(2)B	0.220 2(2)	Mn(1)-O(4)A	0.213 4(2)
Mn(1)-O(4)C	0.213 4(2)	Mn(1)-O(8)	0.223 1(3)	Mn(1)-O(8)B	0.223 1(3)
O(1)-Mn(1)-O(7)	99.47(10)	O(1)-Mn(1)-O(5)A	90.87(10)	O(7)-Mn(1)-O(5)A	163.79(9)
O(1)-Mn(1)-N(1)A	103.66(9)	O(7)-Mn(1)-N(1)A	91.28(9)	O(5)A-Mn(1)-N(1)A	74.06(9)
O(1)-Mn(1)-N(2)	86.36(10)	O(7)-Mn(1)-N(2)	93.64(10)	O(5)A-Mn(1)-N(2)	99.48(10)
N(1)A-Mn(1)-N(2)	167.97(11)	O(1)-Mn(1)-N(3)	156.17(10)	O(7)-Mn(1)-N(3)	88.70(10)
O(5)A-Mn(1)-N(3)	86.72(10)	N(1)A-Mn(1)-N(3)	98.46(10)	N(2)-Mn(1)-N(3)	70.71(10)
O(4)C-Mn(2)-O(2)	87.09(9)	O(4)A-Mn(2)-O(2)	92.91(9)	O(4)C-Mn(1)-O(8)B	93.19(9)
O(4)A-Mn(1)-O(8)B	86.81(9)	O(2)-Mn(1)-O(8)B	89.65(9)	O(2)-Mn(1)-O(8)	90.35(9)

Symmetry codes: A: $-x+1$, $-y$, $-z+1$ for **1**; A: x, $y+1$, z; B: $-x$, $-y+1$, $-z$; C: $-x$, $-y$, $-z$ for **2**.

Table 3 Hydrogen bond parameters of compound 1

D–H···A	*d*(D-H) / nm	*d*(H···A) / nm	*d*(D···A) / nm	∠DHA / (°)
O(4)–H(4)···O(9)A	0.082	0.168	0.248 2	163.0
O(12)–H(12)···O(8)B	0.082	0.180	0.254 7	151.1
O(13)–H(1W)···O(9)C	0.085	0.175	0.259 7	179.8
O(13)–H(2W)···O(5)	0.085	0.177	0.262 2	179.7
O(14)–H(3W)···O(3)D	0.085	0.195	0.280 5	179.3

Symmetry codes: A: $x-1$, $y-1$, z; B: $-x+1$, $-y+1$, $-z$; C: $x-1$, y, z; D: $x+1$, $y+1$, z.

Table 4 Hydrogen bond parameters of compound 2

D–H···A	*d*(D-H) / nm	*d*(H···A) / nm	*d*(D···A) / nm	∠DHA / (°)
O(7)–H(1W)···O(6)A	0.086	0.198	0.276 4	151.5
O(7)–H(2W)···O(9)B	0.085	0.184	0.268 8	179.2
O(8)–H(3W)···O(3)C	0.090	0.209	0.286 5	143.5

Symmetry codes: A: $x-1$, $y+1$, z; B: $x-1$, y, z; C: $x+1$, $y+1$, z.

that compound **1** crystallizes in the triclinic space group $P\bar{1}$. Its asymmetric unit contains two crystallographically unique Ni(Ⅱ) atoms, two $Hbptc^{2-}$ blocks, three phen moieties, one H_2O ligand and two lattice water molecules. As depicted in Fig.1, the six-coordinated Ni1 atom displays a distorted octahedral $\{NiN_4O_2\}$ geometry filled by two carboxylate O atoms from two different μ_3-$Hbptc^{2-}$ blocks and four N atoms from two phen ligands. The Ni2 center is coordinated by one carboxylate O atom from one μ_3-$Hbptc^{2-}$ block, two carboxylate O atoms from one terminal $Hbptc^{2-}$ block, one O atom from the H_2O ligand, and two N atoms from one phen moiety, thus composing distorted octahedral $\{NiN_2O_4\}$ geometry. The lengths of the Ni-O bonds range from 0.202 8(4) to 0.221 2(4) nm, whereas the Ni-N distances vary from 0.205 9(5) to 0.212 2(4) nm; these bonding parameters are comparable to those found in other reported Ni(Ⅱ) compounds[7,9,11]. In **1**, the $Hbptc^{2-}$ ligands adopt two different coordination modes (modes Ⅰ and Ⅱ, Scheme 1), in which the deprotonated carboxylate groups show the monodentate, bidentate or uncoordinated modes. The dihedral angles between two phenyl rings in the $Hbptc^{2-}$ are 52.52° and 39.91°, respectively. Two μ_3-$Hbptc^{2-}$ ligands bridge alternately neighboring Ni(Ⅱ) ions to form a discrete tetranuclear nickel(Ⅱ) structure (Fig.2). These Ni_4 units are assembled to a 3D supramolecular framework through O–H···O hydrogen bond (Fig.3 and Table 3).

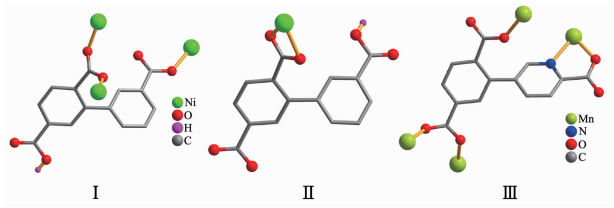

Scheme 1　Coordination modes of $Hbptc^{2-}$/$cptc^{3-}$ ligands in compounds **1** and **2**

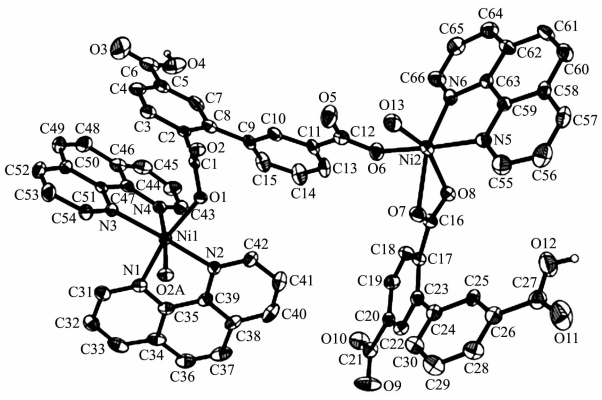

H atoms and lattice water molecules were omitted for clarity except those of COOH groups; Symmetry codes: A: $-x+1, -y, -z+1$

Fig.1　Drawing of the asymmetric unit of compound **1** with 30% probability thermal ellipsoids

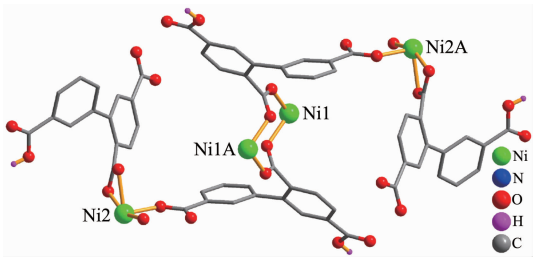

Phen ligands are omitted for clarity; Symmetry codes: A: $-x+1, -y, -z+1$

Fig.2　Tetranuclear nickel(Ⅱ) unit

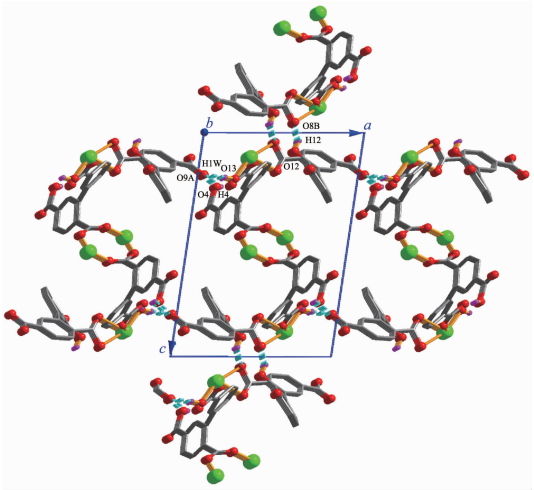

Phen ligands are omitted for clarity; Dotted lines represent the H-bonds; Symmetry codes: A: $x-1, y-1, z$; B: $-x+1, -y+1, -z$

Fig.3　Perspective of 3D supramolecular framework viewed from b axis in **1**

2.1.2　$\{[Mn_3(\mu_4\text{-cptc})_2(2,2'\text{-bipy})_2(H_2O)_4]\cdot 2H_2O\}_n$ (**2**)

The asymmetric unit of **2** consists of two crystallographically distinct Mn(Ⅱ) atoms (Mn1 with full occupancy; Mn2 is positioned on a twofold rotation axis), one μ_4-$cptc^{3-}$ block, one 2,2′-bipy ligand, two coordinated and one lattice water molecule. As shown in Fig.4, six-coordinate Mn1 atom reveals distorted octahedral $\{MnN_3O_3\}$ environment, filled by one N and two O atoms from three individual μ_4-$cptc^{3-}$ blocks, one O atom from the H_2O ligand, and two N atoms from the 2,2′-bipy moiety. The Mn2 center is coordinated

by four carboxylate O atoms from four distinct $cptc^{3-}$ moieties and two O atoms from two H_2O ligands, thus forming octahedral $\{MnO_6\}$ geometry. The Mn-O distances range from 0.210 2(2) to 0.223 1(3) nm, whereas the Mn-N distances vary from 0.226 7(3) to 0.232 3(3) nm; these bonding parameters are comparable to those observed in other Mn(Ⅱ) compounds[7-9,11]. In **2**, the $cptc^{3-}$ block acts as a μ_4-N,O_4-spacer and its COO^- groups take a monodentate or bidentate mode (mode Ⅲ, Scheme 1). In $cptc^{3-}$, a dihedral angle (between pyridyl and benzene rings) is 52.30°. Three

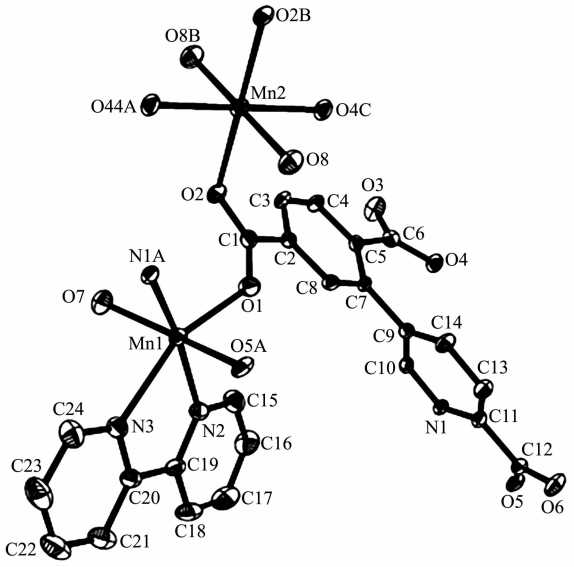

H atoms were omitted for clarity; Symmetry codes: A: x, $y+1$, z; B: $-x$, $-y+1$, $-z$; C: $-x$, $-y$, $-z$

Fig.4 Drawing of the asymmetric unit of compound **2** with 30% probability thermal ellipsoids

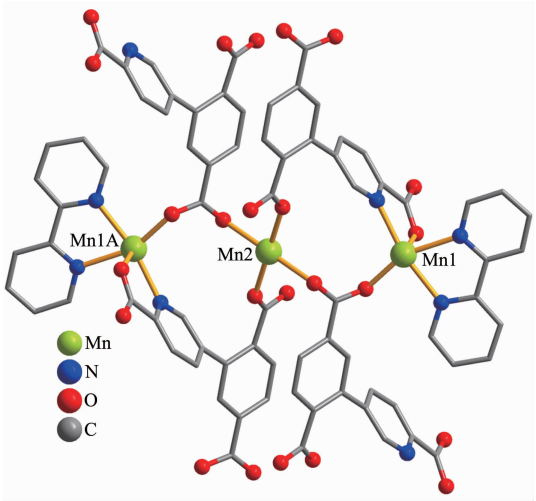

Symmetry codes: A: $-x$, $-y+1$, $-z$

Fig.5 Trinuclear Mn(Ⅱ) unit in compound **2**

neighboring Mn(Ⅱ) ions are bridged by four different μ_4-$cptc^{3-}$ ligands, giving rise to a centrosymmetric trinuclear Mn(Ⅱ) subunit with the Mn⋯Mn distance of 0.508 4(6) nm (Fig.5). The adjacent Mn_3 subunits are further linked by the $cptc^{3-}$ blocks into a 1D chain (Fig.6), having the shortest distance of 1.023 4(5) nm between the neighboring trimanganese(Ⅱ) subunits.

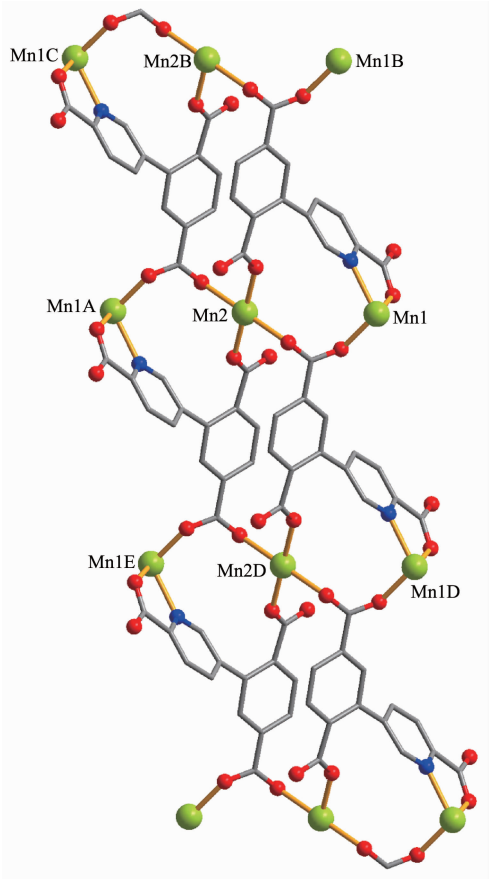

2,2′-bipy ligands are omitted for clarity; Symmetry codes: A: $-x$, $-y+1$, $-z$; B: x, $y+1$, z; C: $-x$, $-y+2$, $-z$; D: x, $y-1$, z; E: $-x$, $-y$, $-z$

Fig.6 One dimensional chain along a axis in compound **2**

2.2 TGA analysis

To determine the thermal stability of compounds **1** and **2**, their thermal behaviors were investigated under nitrogen atmosphere by thermogravimetric analysis (TGA). As shown in Fig.7, compound **1** loses its four lattice and two coordinated water molecules in the range of 152~241 ℃ (Obsd. 3.9%, Calcd. 4.2%), followed by the decomposition at 325 ℃. The TGA curve of **2** reveals that two lattice and four coordinated water molecules are released between 98~238 ℃ (Obsd. 9.6%, Calcd. 9.4%), and the dehydrated

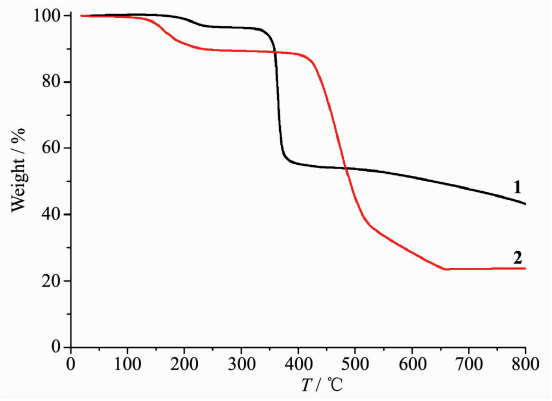

Fig.7　TGA curves of compounds **1** and **2**

solid begins to decompose at 382 ℃.

2.3　Magnetic properties

Variable-temperature magnetic susceptibility studies were carried out on powder samples of **1** and **2** in the 2~300 K temperature range. For **1**, the $\chi_M T$ value at 300 K is 4.08 $cm^3 \cdot mol^{-1} \cdot K$, which is close to the value of 4.00 $cm^3 \cdot mol^{-1} \cdot K$ for four magnetically isolated Ni(Ⅱ) center (S_{Ni}=1, g=2.0). Upon cooling, the $\chi_M T$ value drops down very slowly from 4.08 $cm^3 \cdot mol^{-1} \cdot K$ at 300 K to 3.64 $cm^3 \cdot mol^{-1} \cdot K$ at 60 K, and then decreases steeply to 1.40 $cm^3 \cdot mol^{-1} \cdot K$ at 2 K (Fig.8). In the 8~300 K interval, the χ_M^{-1} vs T plot for **1** obeys the Curie-Weiss law with a Weiss constant θ of −6.52 K and a Curie constant C of 4.15 $cm^3 \cdot mol^{-1} \cdot K$, suggesting a weak antiferromagnetic interaction between the Ni(Ⅱ) ions.

We tried to fit the magnetic data of **1** using the following expression[18] for a dinuclear Ni(Ⅱ) unit:

$$H=-JS_1S_2$$

$$\chi_{M'}=\frac{N\beta^2 g^2}{3k(T-\theta)}\frac{\sum S'(S'+1)(2S'+1)e^{-E(S')/(kT)}}{\sum(2S'+1)e^{-E(S')/(kT)}} \quad (1)$$

$$\chi_M=\chi_{M'}(1-\rho)+\frac{4S(S+1)N\beta^2 g^2\rho}{3kT}+\mathrm{TIP} \quad (2)$$

where ρ is a paramagnetic impurity fraction and TIP is temperature independent paramagnetism. Using this model, the susceptibility for **1** above 60 K was simulated, leading to the values of J=−2.25 cm^{-1}, g=2.10, ρ=0.010, and TIP =4.58×10^{-6} $cm^3 \cdot mol^{-1}$, with the agreement factor $R=\sum(T_{obs}-T_{calc})^2/\sum(T_{obs})^2=6.14\times10^{-4}$. The negative J parameter confirms that a weak antiferromagnetic exchange coupling exists between the adjacent Ni(Ⅱ) centers, which is in agreement with a negative θ value.

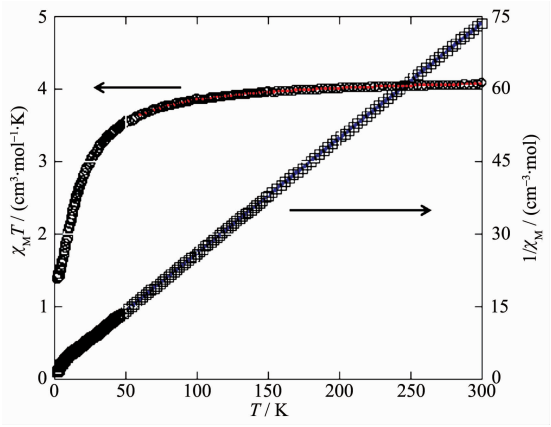

Red curve represents the best fit to the equations in the text; Blue line shows the Curie-Weiss fitting

Fig.8　Temperature dependence of $\chi_M T$ (○) and $1/\chi_M$(□) vs T for compound **1**

For **2**, the $\chi_M T$ value at 300 K is 13.41 $cm^3 \cdot mol^{-1} \cdot K$, which is close to the value of 13.12 $cm^3 \cdot mol^{-1} \cdot K$ expected for three magnetically isolated high-spin Mn(Ⅱ) centers (S_{Mn}=5/2, g=2.0). Upon cooling, the $\chi_M T$ value drops down very slowly from 13.41 $cm^3 \cdot mol^{-1} \cdot K$ at 300 K to 12.60 $cm^3 \cdot mol^{-1} \cdot K$ at 70 K and then decreases steeply to 2.81 $cm^3 \cdot mol^{-1} \cdot K$ at 2 K (Fig.9). The χ_M^{-1} vs T plot for **2** in the 2~300 K interval obeys the Curie-Weiss law with a Weiss constant θ of −4.34 K and a Curie constant C of 13.59 $cm^3 \cdot mol^{-1} \cdot K$. The negative value of θ and the decrease of the $\chi_M T$ should be attributed to the overall antiferromagnetic coupling between the Mn(Ⅱ) centers within the Mn_3 unit. According to the structure of compound **2**, there is one set of magnetic exchange pathway within the trinuclear cluster via carboxylate bridge (Fig.5). We tried to fit the magnetic data of **2** using the following expression[19-20] for the linear trinuclear Mn(Ⅱ) motif:

$$\hat{H}=-2\sum_{i=1}^{n}\sum_{j>1}^{n}J_{ij}\vec{S}_i\vec{S}_j$$

$$\hat{H}=-2J_{12}\vec{S}_1\vec{S}_2-2J_{23}\vec{S}_2\vec{S}_3-2J_{13}\vec{S}_1\vec{S}_3$$

$$\chi=\frac{N\beta^2 g^2}{3kT}\frac{\sum_{S_T}S_T(S_T+1)(2S_T+1)e^{-E(S_T)/(kT)}}{\sum_{S_T}(2S_T+1)e^{-E(S_T)/(kT)}} \quad (3)$$

$$\chi_m=\frac{\chi}{1-[2zJ'/(Ng^2\beta^2)]\chi} \quad (4)$$

where S_T is tolal spin of the linear trinuclear Mn(Ⅱ) motif; $J_{12}=J_{23}=J_1$, $J_{13}=J_2$ (J_{12} and J_{23} are the exchange interactions between the "central" Mn(Ⅱ) and two "outer" Mn(Ⅱ) atoms; J_2 is the exchange interaction between the "outer" Mn(Ⅱ) ions within a Mn_3 unit), zJ' refers to the intercluster coupling constant in the 1D chain. This model gives satisfactory results with the superexchange parameters: J_1/k_B=−1.32 K, J_2/k_B=−0.41 K, zJ'/k_B=−0.20 K, and g=2.02. The agreement factor defined by $R=\sum(\chi_m T_{exp}-\chi_m T_{calc})^2/\sum(\chi_m T_{exp})^2$ is 7.54×10^{-4}. These values confirm the presence of antiferromagnetic interaction between the Mn(Ⅱ) ions within a trinuclear subunit. The inercluster magnetic interaction (zJ') is rather small, indicating that the exchange interactions between two magnetic clusters are very weak, which is probably due to a long separation (1.023 4(5) nm) of the adjacent magnetic subunits. In compounds **1** and **2**, there is one type of the magnetic exchange pathway within the Ni_4 and Mn_3 units, namely via double μ_2-η^1 :η^1-carboxylate (*syn-syn*) bridges (Fig.2 and 5).

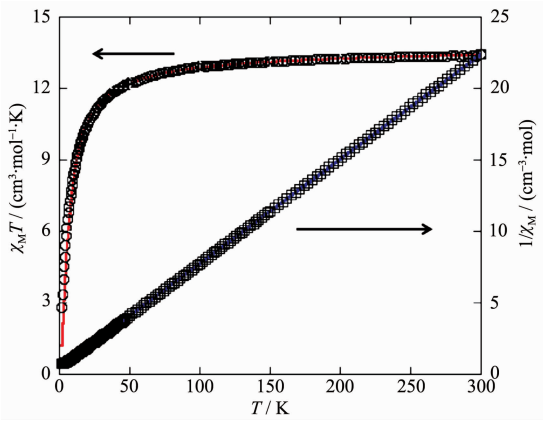

Red curve represents the best fit to the equations in the text; Blue line shows the Curie-Weiss fitting

Fig.9 Temperature dependence of χ_MT (○) and $1/\chi_M$(□) vs T for compound **2**

3 Conclusions

In summary, two new coordination compounds, namely $[Ni_2(\mu_3\text{-Hbptc})(Hbptc)(phen)_3(H_2O)]_2\cdot4H_2O$ (**1**) and $\{[Mn_3(\mu_4\text{-cptc})_2(2,2'\text{-bipy})_2(H_2O)_4]\cdot2H_2O\}_n$ (**2**), have been synthesized under hydrothermal conditions. The compounds feature the 0D tetranuclear and 1D chain structures, respectively. Magnetic studies show an antiferromagnetic coupling between the adjacent metal centers.

References:

[1] Huang Y B, Liang J, Wang X S, et al. *Chem. Soc. Rev.*, **2017**,**46**:126-157

[2] Meng X, Wang H N, Song S Y, et al. *Chem. Soc. Rev.*, **2017**, **46**:464-480

[3] Wen H M, Cui Y J, Zhou W, et al. *Adv. Mater.*, **2016**,**28**: 8819-8860

[4] Cui Y, Yue Y, Qian G, et al. *Chem. Rev.*, **2012**,**112**:1126-1162

[5] Kuppler R J, Timmons D. J, Fang Q R, et al. *Coord. Chem. Rev.*, **2009**,**253**:3042-3066

[6] Ji P F, Manna K, Lin Z, et al. *J. Am. Chem. Soc.*, **2016**,**138**: 12234-12242

[7] Gu J Z, Cui Y H, Liang X X, et al. *Cryst. Growth Des.*, **2016**, **16**:4658-4670

[8] Gu J Z, Gao Z Q, Tang Y. *Cryst. Growth Des.*, **2012**,**12**:3312-3323

[9] Gu J Z, Wu J, Lv D Y, et al. *Dalton Trans.*, **2013**,**42**:4822-4830

[10]Du M, Li C P, Liu C S, et al. *Coord. Chem. Rev.*, **2013**,**257**: 1282-1305

[11]Gu J Z, Liang X X, Cui Y H, et al. *CrystEngComm*, **2017**, **19**:117-128

[12]Lee J, Kang Y J, Cho N S, et al. *Cryst. Growth Des.*, **2016**, **16**:996-1004

[13]Li S D, Lu L P, Su F. *Chin. J. Struct. Chem.*, **2016**,**35**:1920-1928

[14]FENG Shang-Fa(冯上发), HE Xin(何鑫), QIN Tao(秦涛), et al. *Chinese J. Inorg. Chem.*(无机化学学报), **2017**,**33**(11): 2095-2102

[15]Su F, Lu L P, Feng S S, et al. *Dalton Trans.*, **2015**,**44**:7213-7222

[16]Tian H, Wang K, Jia Q X, et al. *Cryst. Growth Des.*, **2011**, **11**:5167-5170

[17]Spek A L. *Acta Crystallogr. Sect. C: Struct. Chem.*, **2015**, **C71**:9-18

[18]Thompson L K, Niel V, Grove H. *Polyhedron*, **2004**,**23**:1175-1184

[19]Kahn O. *Molecular Magnetism*. New York: VCH Publishers Inc., **1993**:211

[20]Hsu K F, Wang S L. *Inorg. Chem.*, **2000**,**39**:1773-1778